

Evolution of the ferromagnetic phase of ultrathin Fe films grown on GaAs(100)- 4×6

Y. B. Xu, E. T. M. Kernohan, D. J. Freeland, A. Ercole, M. Tselepi, and J. A. C. Bland

Cavendish Laboratory, University of Cambridge, Cambridge CB3 0HE, United Kingdom

(Received 10 December 1997)

Epitaxial bcc Fe has been grown on GaAs(100)-(4×6) at room temperature and studied with *in situ* magneto-optical Kerr effect (MOKE), low-energy electron diffraction, and alternating gradient field magnetometry (AGFM). The magnetic properties at room temperature were found to proceed via three phases; a nonmagnetic phase for the first three and a half monolayers, a short-range-ordered superparamagnetic phase, and a ferromagnetic phase above about five monolayers. The thickness dependencies of the coercivity and MOKE intensity further suggested that the ferromagnetic phase is subdivided into three distinct regimes with different magnetic properties. A combination of the *in situ* MOKE and *ex situ* AGFM measurements shows that the *entire* Fe film is ferromagnetic with a bulklike moment after the onset of the ferromagnetism, in contrast with previous studies, in which magnetic dead layers or half-magnetization phases due to the intermixing of Fe and As were proposed. The results show that it is the growth morphology of the ultrathin films, rather than the diffusion of As, that plays the dominant role in determining the magnetic properties in this system. [S0163-1829(98)04127-7]

INTRODUCTION

Fe on GaAs continues to be of interest as a model system for the epitaxial growth of ferromagnetic metals (FM) on semiconductors. It has been shown previously by several groups¹⁻⁵ that bcc Fe grows epitaxially on both the (001) and (011) surfaces of GaAs, due in part to the fact that the lattice constant of bcc Fe ($a_0 = 2.866 \text{ \AA}$) is almost exactly half that of GaAs ($a_0 = 5.654 \text{ \AA}$). Fe/GaAs is also of current interest due to its potential for use in magnetoelectronic devices such as FM spin injection pads.^{6,7} Such spin-sensitive devices require well-defined and magnetic interface layers. However, a strong reduction of the magnetization has previously been found for Fe grown on GaAs.¹ The reduction of the Fe moment was attributed to the magnetically "dead" layers near the interface, which would be detrimental to the spin-dependent transmission and tunneling between the ferromagnetic metal and the semiconductor substrate. Thus the interface structure and magnetism is a key issue for current research.

The magnetic hysteresis loops measured using *in situ* magneto-optical Kerr effect (MOKE) by Gester *et al.*⁸ showed that the ferromagnetic phase developed after about 15 \AA ($\sim 10 \text{ ML}$) when Fe was grown on GaAs(001)-(4×6) at $175 \text{ }^\circ\text{C}$. Kneedler *et al.*⁵ showed that the onset of ferromagnetism occurred at 6 ML when Fe was grown on both GaAs(001)-(2×4) and $c(4\times 4)$ substrates. The magnetic dead layer in Fe/GaAs was attributed to the formation of antiferromagnetic Fe_2As microstructures at the interface due to the As diffusion.¹ More recently, *ex situ* magnetic measurements⁴ using a superconducting quantum interference device and alternating gradient field magnetometry (AGFM) suggested the existence of a nearly half-magnetized phase $\text{Fe}_3\text{Ga}_{2-x}\text{As}_x$ at the interface instead of dead layers. To prevent the formation of compounds at the Fe/GaAs interface, S-passivated GaAs substrates have been exploited.⁹ These have 1 ML of bridge bonded sulphur that acts as a surfactant to inhibit interdiffusion of As into the Fe over-

layer. The Fe films were found to be ferromagnetic after about 4 ML of deposition.

In general, the magnetic properties of the first few monolayers are expected to be determined not only by the intermixing at the interface, but also by the morphology of the substrate and the deposited films. An interesting example is the Co/Cu system. High quality layer-by-layer growth has been achieved on both Cu(001) and Cu(111) substrates and ferromagnetic hysteresis loops were observed at room temperature for less than 2 ML of Co.^{10,11} In contrast, the Co/Cu(110) shows a three-dimensional (3D) growth mode,¹²⁻¹⁴ possibly due to the corrugated Cu(110) surface. The onset of the room-temperature ferromagnetism was found to be at around 4.6 ML, when the islands began to coalesce.¹⁴ Three-dimensional growth (Volmer-Weber mode) has been reported on both Fe/GaAs(001) and (011).¹⁵⁻¹⁷ A detailed low-energy electron diffraction (LEED) study further suggested that a pyramidlike structure forms when Fe was grown on GaAs(100)-(4×6),¹⁸ similar to the pyramids observed in the Fe/MgO system.¹⁹ These "self-organized" structures are interesting from the viewpoint of understanding the micromagnetism of nanoclusters and the evolution of magnetic phases. For example, superparamagnetic relaxation has been studied for a 10-ML film of Fe grown on MgO(001),²⁰ and related to the particle size. Also, the nanoscale structure of pseudomorphic Fe(110) on W(110) was found to induce a rich variety of new micromagnetic phenomena.²¹ Technologically, these nanostructures may have future applications in ultra-high-density data storage.

Although the Fe/GaAs system has been extensively studied, the magnetic properties of the first few monolayers are poorly understood, and there is still debate over whether there are magnetically dead layers at the interface. In this paper, the magnetic properties and structure of Fe grown on GaAs(001)-(4×6) at room temperature have been studied. A picture of the relationships between the Fe coverage, its structure, and the magnetic phases has been proposed using *in situ* MOKE and LEED and *ex situ* AGFM. The results

suggest that there is no dead layer at the interface and that the Fe shows a bulklike moment.

EXPERIMENTS

Fe films were grown on GaAs substrates in a molecular beam epitaxy chamber using an *e*-beam evaporator. During growth, the pressure was below 6×10^{-10} mbar. The deposition rate was monitored by a quartz microbalance that was calibrated using reflection high-energy electron diffraction oscillations. The Fe film was grown at ambient temperature (35 °C) at a rate of approximately 1 ML per min. The substrates used in this study are As capped GaAs(001) prepared in another UHV chamber. A buffer layer ($\sim 0.5 \mu\text{m}$) of homoepitaxial GaAs was grown on the commercial wafer to provide the smoothest possible GaAs surface. The As cap layer was then desorbed by annealing for metal film growth. The As capping layer began to desorb at around 340 °C and the substrate was further annealed to 550 °C for 1 h to obtain a clean and ordered surface.

The surface structure of the substrate and the Fe films was determined by means of LEED. Diffraction images were recorded from the phosphor screen using a conventional charge-coupled-device camera. The magnetic properties of the Fe films were studied using *in situ* MOKE. The MOKE loops were collected during growth in the longitudinal geometry using an electromagnet with a maximum field of 2 kOe, and an intensity stabilized HeNe laser (633 nm).²² The magnetization was measured *ex situ* using AGFM with sensitivity up to 10^{-6} emu. The AGFM was calibrated with a built-in coil and further checked against thick Fe and Ni films.

RESULTS

Figure 1 shows the LEED patterns of (a) the GaAs substrate after As desorption, and (b)–(f) after Fe deposition. The LEED picture of the substrate shows a very clear $p(4 \times 6)$ reconstruction, typical for Ga-rich surfaces.²³ This clear and sharp LEED pattern for the reconstructed surface indicates that the GaAs substrate surface is very flat and well crystallized. Auger measurements show that the substrate is free of O and C after As desorption. The LEED patterns were monitored as Fe was deposited. No Fe LEED pattern was observed for the first 4 ML deposited as shown in Fig. 1(b). After the deposition of 5 ML, faint LEED spots from the Fe film appear. Clear LEED patterns were observed after the deposition of 6 ML. The diffraction spots became broadened at higher coverages as shown in Figs. 1(e) and 1(f). The LEED patterns show that Fe grows epitaxially on GaAs(001) at room temperature with the epitaxial relationship $\text{Fe}(001)\langle 100 \parallel \text{GaAs}(001)\langle 100 \rangle$. The lack of Fe LEED patterns for the first 4 ML indicates that the growth proceeds via the three-dimensional Volmer-Weber growth mode as previously reported for higher temperature growth.^{1,17,18,24} The LEED pattern develops at a higher Fe coverage (5 ML) than that at higher growth temperature (3 ML).¹⁸ This is consistent with the previous finding that the optimum growth temperature is around 170 °C.^{1,17,18}

Figure 2 shows the development of the MOKE loops with thickness. The magnetic field is applied along the $\langle 011 \rangle$ di-

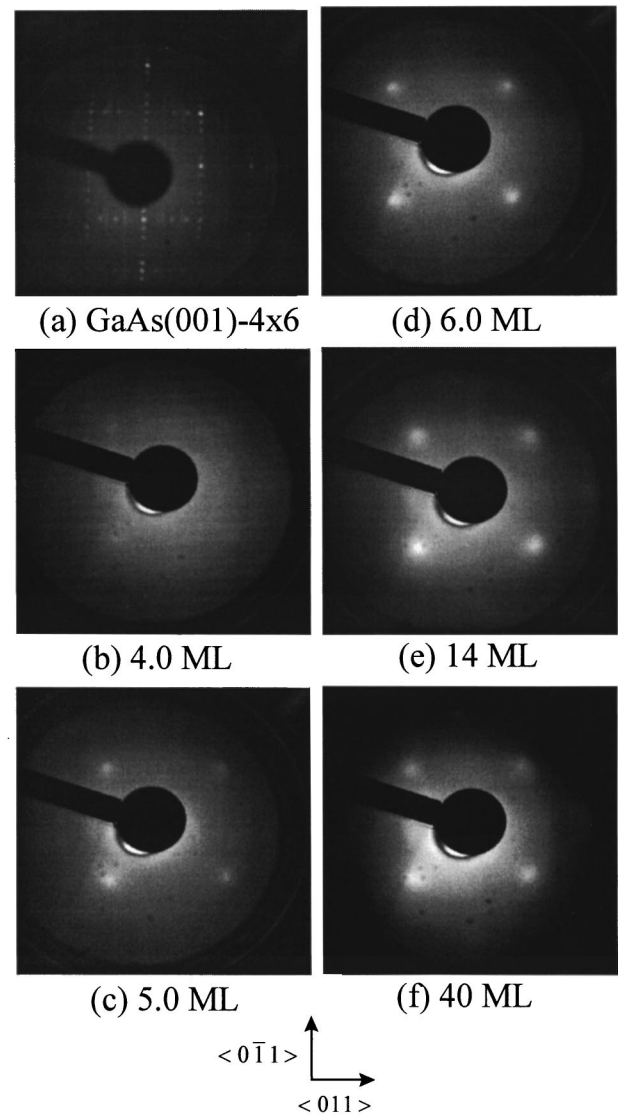


FIG. 1. LEED patterns of (a) the GaAs(001)- 4×6 substrate after As desorption, 135 eV, and (b)–(f) after Fe deposition, 120 eV.

rection. No MOKE signal was observed from the substrate, which showed that the magneto-optical Kerr effect of GaAs is negligible for the applied field strength of up to 2 kOe. A significant MOKE signal was first detected at a thickness of 3.5 ML, with the intensity linearly proportional to the applied magnetic field. With further Fe deposition the MOKE-loop curves become s-shaped at 4.3 ML. The lack of hysteresis indicates that the ferromagnetic phase has not yet developed. The magnetization curves indicate the presence of either paramagnetism or superparamagnetism. The loop in Fig. 2(e) clearly shows hysteresis, indicating the onset of the ferromagnetic phase after 4.8 ML of Fe. Figures 2(f)–2(j) show the hysteresis loops after the onset of the ferromagnetic phase. These loops display the observed variation in the coercivity with thickness, which is plotted in Fig. 3(b).

We note that the hysteresis loops in Figs. 2(c)–2(e) show an asymmetry under the transformation $\mathbf{M} \rightarrow -\mathbf{M}$, $\mathbf{H} \rightarrow -\mathbf{H}$. This might be due to the second-order term in the magneto-optical response. For example, if there is a transverse magnetization component, it will give a contribution in the longitudinal measurements because of the quadratic

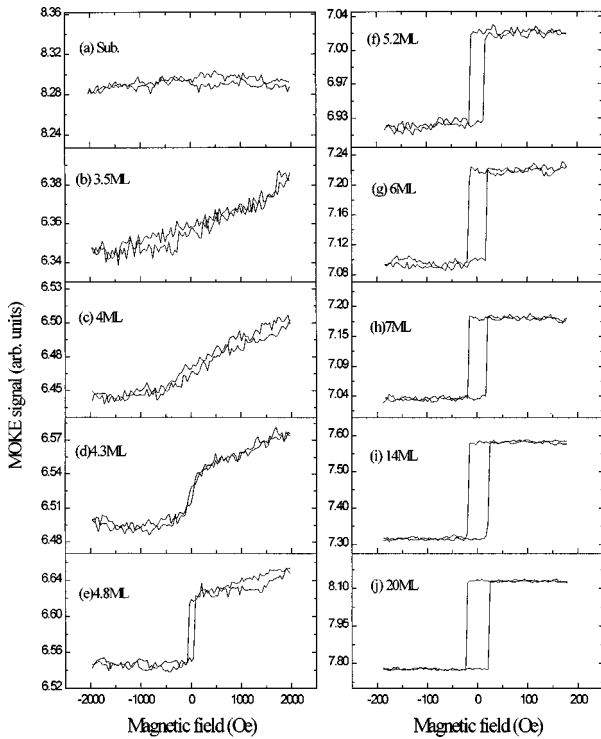


FIG. 2. *In situ* MOKE hysteresis loops for the Fe/GaAs(001)- 4×6 of different Fe thicknesses with the magnetic field applied along the $\langle 0\bar{1}1 \rangle$ direction.

magneto-optical effect. A fuller explanation will require further experimental and theoretical investigation, which is beyond the scope of this paper.

Figure 2 indicates that the magnetic easy axis is along the $\langle 0\bar{1}1 \rangle$ direction rather than along the $\langle 001 \rangle$ direction, the easy axis of the bulk bcc Fe. This is due to a strong uniaxial anisotropy. Although this uniaxial anisotropy has been observed in several previous studies,^{1,5,8} its origin remains an open question. It might be due to the shape anisotropy, anisotropic strain relaxation, or the different nature of the Fe-Ga and Fe-As bonds. The uniaxial anisotropy has also been examined here, although systematic studies were not attempted and we do not attempt to answer this interesting question. Figure 3 shows the hysteresis loops of the Fe films of (a), (b) 5 ML and (c), (d) 40 ML for the magnetic field applied along the $\langle 0\bar{1}1 \rangle$ and $\langle 011 \rangle$ directions, respectively. Figure 3 shows that the uniaxial anisotropy develops immediately after the onset of the ferromagnetic phase at around 5 ML and persists up to 40 ML.

It has been shown that for ultrathin ferromagnetic films the Kerr effect initially depends linearly on the thickness if the magnetization is thickness independent.²⁵ Calculations of the magneto-optic response of Fe films supported by GaAs predict a near linear dependence up to at least 40 ML.²⁶ The MOKE signal from the detector is proportional to the Kerr effect, the intensity of the light, and the setting of the polarimeter. During *in situ* experiments that monitor the thickness

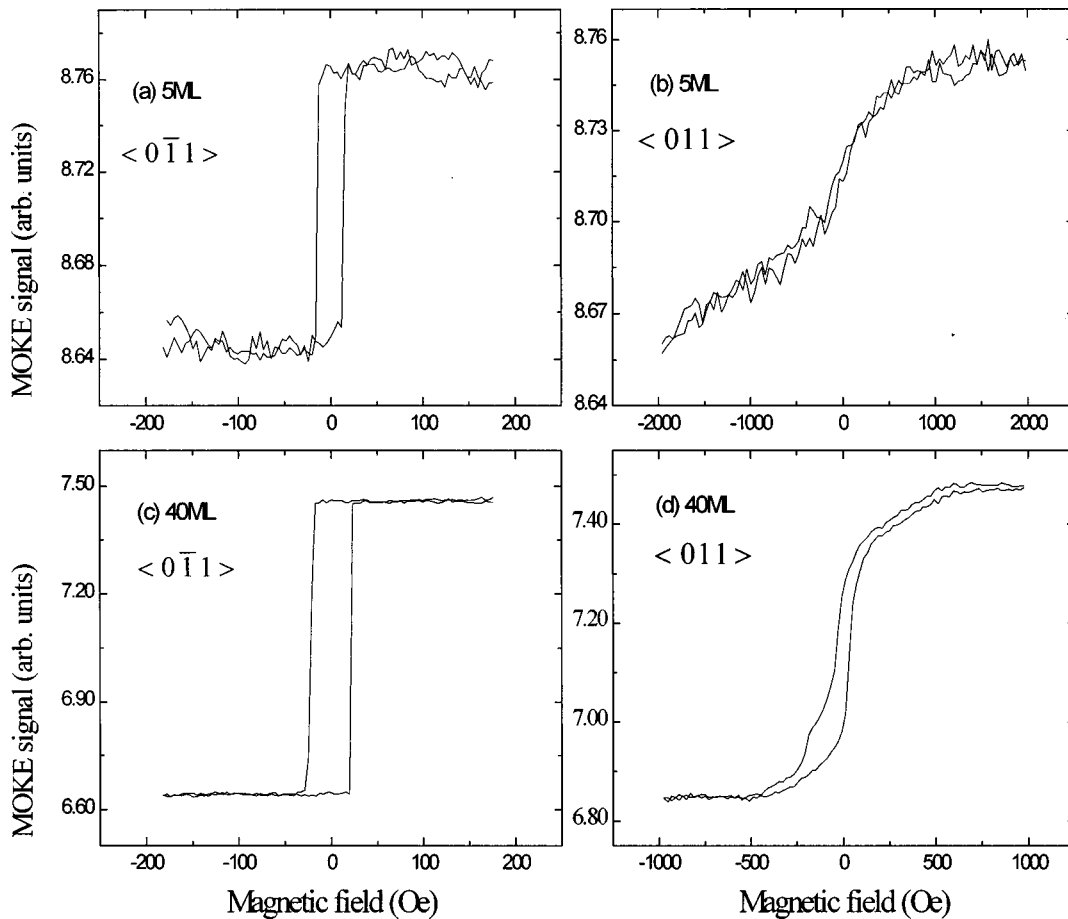


FIG. 3. *In situ* MOKE hysteresis loops of (a), (b) Fe(5 ML)/GaAs(001), and (c), (d) Fe(40 ML)/GaAs(001) for the magnetic field applied along the $\langle 0\bar{1}1 \rangle$ and $\langle 011 \rangle$ directions, respectively.

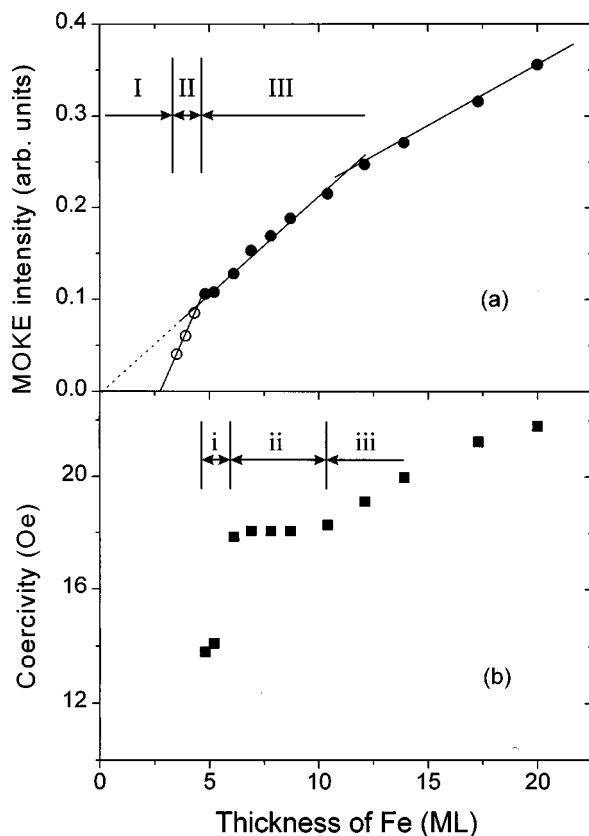


FIG. 4. Thickness dependencies of the MOKE intensity and the coercivity of Fe/GaAs(001)- 4×6 . The open dots are the results for the superparamagnetic phase in an applied field of 2 kOe, and the filled dots are the saturated MOKE intensity of the ferromagnetic phase. The error bars (not shown) are comparable with the size of the data symbols.

dependence of the MOKE intensity, care was taken not to move either the sample or any of the optical components, so eliminating the possibility of variations in intensity due to changes in the optical alignment. The magnet was moved away from the sample position during growth to avoid any change of the deposition rate caused by the stray field. After each deposition, the magnet was moved back for the measurement while keeping the sample position unchanged.

The thickness dependence of the MOKE intensity is shown in Fig. 4(a). The empty and filled circles are the results before and after the onset of the ferromagnetic phase, respectively. Figure 4(a) shows that the MOKE intensity increases rapidly between 3.5 and 4.3 ML, just before the onset of the ferromagnetism. Extrapolation of these points indicates that the thickness of the nonmagnetic phase is about 3.2 ± 0.2 ML. After the onset of ferromagnetism, the MOKE signal is approximately linearly proportional to the thickness as shown by the filled circles. Extrapolation of these solid dots suggests that there are no magnetically dead layers, and that the entire Fe film is ferromagnetic. The MOKE signal at higher coverage (above about 12 ML) shows a slightly reduced slope. The thickness dependence of the coercivity is shown in Fig. 3(b). The coercivities are rather small just after the onset of the ferromagnetism. There is a sharp increase of the coercivity around 5 ML. From about 6 to 10 ML, it is almost constant and then increases slightly with further increasing thickness.

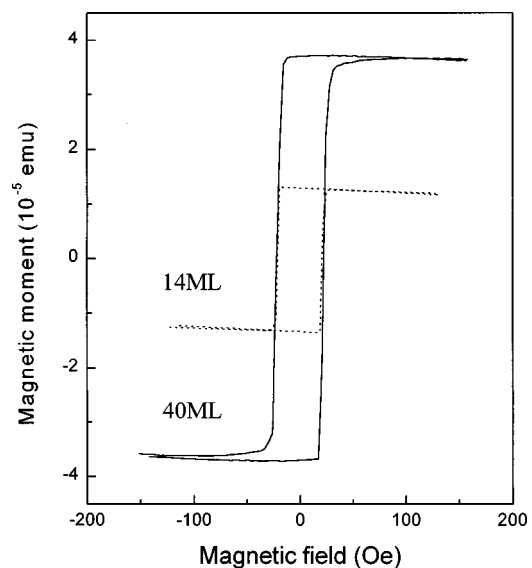


FIG. 5. Magnetization hysteresis loops of Fe(14 ML)/GaAs(001) and Fe(40 ML)/GaAs(001) measured using AGFM with the magnetic field applied along the $\langle 011 \rangle$ direction.

Although the MOKE signal is proportional to the magnetization, it does not directly give the magnetic moment of the sample. This was measured using AGFM. In carrying out these measurements, the samples were capped with Au to prevent oxidation. The thicknesses of the samples grown for the AGFM measurements were chosen not to be very small in order to minimize the effect of the Fe/Au interface and the diamagnetic signal of the substrate. As indicated by the *in situ* MOKE results in Fig. 4(a), the magnetization does not vary strongly with thickness after the onset of the ferromagnetism. Figure 5 shows the magnetization hysteresis loops of two samples; Fe(14 ML)/GaAs(001) and Fe(40 ML)/GaAs(001). The total magnetic moment from the 40 ML of Fe is about 2.8 times bigger than that from the 14 ML, which is in proportion to their thicknesses. The magnetization of the films is $1.6 \pm 0.2 \times 10^3$ emu/cm³, only slightly smaller than that of the bulk bcc Fe (1.71×10^3 emu/cm³). The AGFM measurements further show that the magnetization is approximately thickness independent and the Fe films have a bulklike moment.

DISCUSSION

These above results are of interest in the context of two controversial questions concerning the basic magnetic properties of the ultrathin Fe films grown on GaAs. First, is there any dead layer or half-magnetization phase near the Fe/GaAs interface? The lack of magnetization for coverages less than 3.5 ML may be due to the intermixing of Fe with As and Ga and the formation of nonferromagnetic compounds near the interface region,^{1,8} or it could be due to the formation of clusters. As we mentioned in the introduction, the ferromagnetic phase develops after more than 4 ML of deposition in the Co/Cu(110) system due to the 3D growth.¹⁴ Second, is there local ferromagnetic ordering before the onset of the ferromagnetic phase? The magnetization signal before the onset of the ferromagnetism could, in principle, be due to either a paramagnetic response or superparamagnetism.

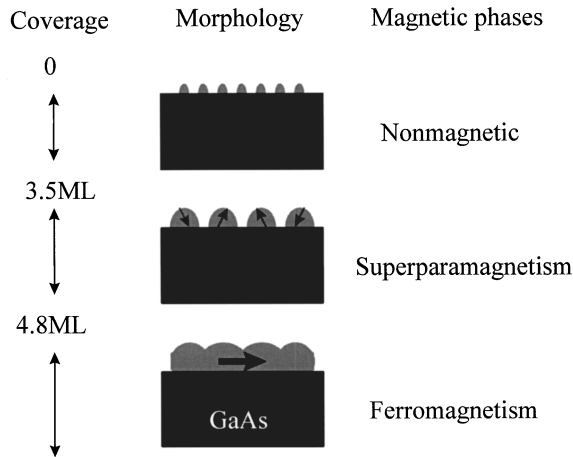


FIG. 6. A picture of the correlation between the coverage, morphology, and magnetic phases of Fe films on GaAs(001)- 4×6 substrate grown at the room temperature.

In combination with the structural information obtained from LEED, we propose that the correlation between the coverage, morphology, and magnetic phases is as shown in Fig. 6. The lack of the Fe LEED patterns suggests that the films are not continuous below 4 ML and that clusters are formed in the early stages of growth. Chambers *et al.*²⁴ showed that Fe clusters with at least 3 ML height grew on $c(8\times 2)$ reconstructed GaAs(100) for coverage up to about 4 ML. This 3D growth mode of the Fe/GaAs system has been confirmed by scanning tunnel microscope (STM) images,^{16,17} though most of these STM studies mainly concentrated on the submonolayer coverage range. The lack of magnetic signal for the first 3.5 ML might be due to the smaller initial cluster size, which prevents the development of magnetic ordering, or the ordering above room temperature. As more Fe is deposited, the islands will grow and coalesce to form bigger clusters. The exchange interaction within these clusters becomes stronger and leads to internal ferromagnetic ordering,^{27,28} so giving rise to the well-known superparamagnetic phase.²⁹ The lack of hysteresis is consistent with either superparamagnetism,²⁹ or 2D paramagnetism.³⁰ However, the s-shaped loops that were observed in this region are generally consistent with the Langevin function used to describe the magnetization of superparamagnetic clusters.^{20,29,31} Fitting the curves of Figs. 2(c) and 2(d) within the range of ± 1 kOe with a Langevin function, the average values of the effective magnetic moment per cluster are obtained to be $(1.05\pm 0.15)\times 10^4 \mu_B$ and $(4.40\pm 0.65)\times 10^4 \mu_B$, respectively, for the films of the coverage of 4 and 4.3 ML. Thibado *et al.*¹⁷ found that the average island width \times length of 1 ML of Fe on GaAs(001)- 2×4 is $35\times 90 \text{ \AA}^2$. Gu *et al.*³² imaged a thick Fe film (150 \AA) on GaAs(001)- 4×6 and found that the film has islandlike undulations of about 10 \AA height and about 150 \AA in diameter. Assuming average island sizes of $100\times 100 \text{ \AA}^2$, and height 5 ML (7.15 \AA) for the coverage of about 4 ML, the magnetic moment is $1.43\times 10^4 \mu_B$, which is comparable with the effective moments estimated by fitting the magnetization curves using the Langevin function. Thus we can conclude that a superparamagnetic phase develops in the thickness range 3.5–4.8 ML.

With further increase in the coverage, the islands coalesce

and long-range ferromagnetic ordering develops. The hysteresis loops after the onset of the ferromagnetic phase in Fig. 2 show that the films have a well-defined magnetic coercivity and remnance ratio, indicating the behavior of a continuous film. We should note that long-range ordering (as well as the first appearance of a LEED pattern) may possibly develop before the complete coalescence of the islands due to interparticle interactions. A detailed combination of high-resolution scanning tunneling microscopy and *in situ* MOKE measurements is required to determine exactly the morphology near to the transition.

The magnetic properties of the films after the onset of the ferromagnetism show an interesting three-stage behavior. The coercivities of the films are rather small just after the onset of the ferromagnetism, and rise sharply up to 6 ML. The coercivity then remains almost constant up to 10 ML before increasing slightly with higher coverages. The sharp increase of the coercivity is quite similar to a critical behavior,³³ suggesting that thermal fluctuations are important in the magnetization reversal process just after the onset of the ferromagnetic phase. It has been shown by Schumann and Bland³⁴ that the coercivity follows a power law $H_c(d) \sim (d/d_c - 1)^\alpha$ in the Co/Cu(100) system just after the onset of the ferromagnetic phase. The further increase of the coercivity above about 10 ML may be due to a structural change. It has been shown by Anderson *et al.*³⁵ that the epitaxial quality of the Fe/GaAs(001) degraded after about 12 ML. This is consistent with our LEED measurements (Fig. 1), which show a broadening of the diffraction spots at higher coverages, indicating a reduction of the film quality. It is also interesting to note that the slope of the MOKE intensity decreases slightly in this region. Taken together, these effects suggest that there is indeed a significant change in the structural and magnetic properties after about 10–12 ML.

The critical thickness (4.8 ML) corresponding to the onset of the ferromagnetic phase is much lower than that of the films grown at higher temperature (10 ML),⁸ and is comparable with that of the films grown at room temperature on the S-passivated GaAs substrates, where the onset of the ferromagnetic phase was found to be at about 4.0 ML.⁹ The combination of the MOKE and AGFM shows that the entire Fe films studied here are ferromagnetic with a bulklike moment. This is very different from the results of previous studies, where *ex situ* magnetic measurements showed a magnetic dead layer of about 16 ML.¹ More recently, this dead layer was attributed to a half-magnetization phase near the interface.⁴ The thickness D of this half-magnetization phase depends on the growth temperature T , $D\sim 10$ ML for $T=50^\circ\text{C}$ and $D\sim 60$ ML for $T=200^\circ\text{C}$.

These differences demonstrate the importance of the substrate preparation and growth temperature. The sharp LEED image in Fig. 1(a) showing the (4×6) surface reconstruction indicates that the substrate used in this study is well ordered and has a long coherence length. Such a clean and flat GaAs surface would favor the Fe growth. GaAs(001)- 4×6 is a Ga-terminated surface. It might therefore be expected that the interdiffusion of As into the Fe layer would be diminished in the samples grown here, especially since the substrate was held at ambient temperature rather than 150–175 $^\circ\text{C}$. We have used Auger spectroscopy to monitor the interdiffusion of As. The low-energy Fe and As peaks at 46

eV (Fe) and 35 eV (As) have been measured since the energy limit of our Auger system does not allow us to use the high-energy As peaks above 1 kV. The probe depth for these low-energy secondary electrons is very short (7–8 Å, ~5 ML),³⁶ and so using low-energy electrons makes the technique more surface sensitive. The As peak is still present after 40 ML of Fe deposited, showing the out-diffusion of As into Fe.¹ However, the ratio of the Auger intensities of the As peak and Fe peak was found to be almost constant at about $I_{As}/I_{Fe} = 0.15 \pm 0.01$ for thicknesses of 10, 20, and 40 ML. Considering the very short probing depth of the low-energy Auger electrons, the constant ratio suggests that As floats on the surface and does not react with Fe to form nonmagnetic compounds. This is consistent with the bulklike magnetic moment obtained from the magnetic measurements and explains why the first three and half nonmagnetic layers could become ferromagnetic at higher coverages. In view of these results, the larger critical thickness for the onset of ferromagnetism in previous studies⁸ might therefore be due to the reaction of As and Fe at higher growth temperatures.

CONCLUSION

We have studied the magnetic and structural properties of epitaxial bcc Fe grown at room temperature on GaAs(001)-(4×6) substrates. A superparamagnetic phase was observed to develop within a narrow thickness range before the onset

of long-range ferromagnetic ordering. The critical thickness of the ferromagnetic phase is much smaller than that of the structures prepared at higher growth temperatures,⁸ and comparable with that of the S-passivated substrate samples.⁹ The *in situ* MOKE and *ex situ* AGFM results show that the entire film is ferromagnetic with a bulklike moment after the onset of long-range ferromagnetism. These results support the view that there is neither a magnetic dead layer nor a half-magnetization phase at the interface. As a final point, it is worth mentioning that the growth of ferromagnetic metals on semiconductor substrates may offer an opportunity to study the micromagnetism of nanostructures and the associated critical phenomena of phase transitions, which have recently attracted considerable attention on the ferromagnetic/nonmagnetic {Fe/W,²¹ Co/Cu,³⁷ and Fe/Cu (Ref. 38)} systems. The magnetically active nanoclusters of Fe on GaAs may find applications, as the dipole fields from these mesomagnets offer a natural way to generate magnetic fields for nanoscale semiconductor devices,^{39,40} and the high interface moment is favorable for magnetoelectronic applications.

ACKNOWLEDGMENTS

We gratefully acknowledge the financial support of the EPSRC, and ESPRIT (EC). We thank Dr. D. A. Ritchie and R. Balsod for their help with this work.

-
- ¹G. A. Prinz, G. T. Rado, and J. J. Krebs, *J. Appl. Phys.* **53**, 2087 (1982); J. J. Krebs, B. T. Jonker, and G. A. Prinz, *ibid.* **61**, 2596 (1987).
- ²J. M. Florczak and E. D. Dahlberg, *Phys. Rev. B* **44**, 9338 (1991).
- ³C. Daboo, R. J. Hicken, E. Gu, M. Gester, S. J. Gray, D. E. P. Eley, E. Ahmad, and J. A. C. Bland, *Phys. Rev. B* **51**, 15 964 (1995).
- ⁴A. Filipe, A. Schuhl, and P. Galtier, *Appl. Phys. Lett.* **70**, 129 (1997).
- ⁵E. M. Kneedler, B. T. Jonker, P. M. Thibado, R. J. Wagner, B. V. Shanabrook, and L. J. Whitman, *Phys. Rev. B* **56**, 8163 (1997).
- ⁶S. Datta and B. Das, *Appl. Phys. Lett.* **56**, 665 (1990).
- ⁷G. A. Prinz, *Phys. Today* **48** (4), 58 (1995).
- ⁸M. Gester, C. Daboo, R. J. Hicken, S. J. Gray, A. Ercole, and J. A. C. Bland, *J. Appl. Phys.* **80**, 347 (1996).
- ⁹G. W. Anderson, M. C. Hanf, and P. R. Norton, *Phys. Rev. Lett.* **74**, 2764 (1995).
- ¹⁰C. M. Schneider, P. Bressler, P. Schuster, J. J. De Miguel, and R. Miranda, *Phys. Rev. Lett.* **64**, 1059 (1990).
- ¹¹D. Kerkmann, D. Pescia, and R. Allenspach, *Phys. Rev. Lett.* **68**, 686 (1992).
- ¹²G. Harp, R. F. C. Farrow, D. Weller, T. A. Rabedeau, and R. F. Marks, *Phys. Rev. B* **48**, 17 538 (1993).
- ¹³J. Fassbender, G. Guntherodt, C. Mathieu, B. Hillebrands, R. Jungblut, J. Kohlhepp, M. T. Johnson, D. J. Roberts, and G. A. Gehring, *Phys. Rev. B* **57**, 5870 (1998).
- ¹⁴S. Hope, Ph.D. thesis, Cambridge University, 1997.
- ¹⁵P. N. First, J. A. Stroschio, R. A. Dragoset, D. T. Pierce, and R. J. Celotta, *Phys. Rev. Lett.* **63**, 1416 (1989).
- ¹⁶H. Takeshita, H. Akinaga, M. Ehinger, Y. Suzuki, K. Ando, and K. Tanaka, *Jpn. J. Appl. Phys., Part 1* **34**, 1119 (1995).
- ¹⁷P. M. Thibado, E. Kneedler, B. T. Jonker, B. P. Bennert, B. V. Shanabrook, and L. J. Whitman, *Phys. Rev. B* **53**, R10 481 (1996).
- ¹⁸M. Gester, C. Daboo, S. J. Gray, and J. A. C. Bland, *J. Magn. Magn. Mater.* **165**, 242 (1997).
- ¹⁹K. Thurmer, R. Koch, M. Weber, and K. H. Rieder, *Phys. Rev. Lett.* **75**, 1767 (1995).
- ²⁰Yongsup Park, S. Adenwalla, G. P. Felcher, and S. D. Bader, *Phys. Rev. B* **52**, 12 779 (1995).
- ²¹N. Weber, K. Wagner, H. J. Elmers, J. Hauschild, and U. Gradmann, *Phys. Rev. B* **55**, 14 121 (1997).
- ²²J. A. C. Bland, M. J. Padgett, R. J. Butcher, and M. Bett, *J. Phys. E* **22**, 308 (1989).
- ²³R. Z. Bachrach, R. S. Bauer, P. Chiaradia, and G. V. Hanson, *J. Vac. Sci. Technol.* **18**, 797 (1981).
- ²⁴S. A. Chambers, F. Xu, H. W. Chen, I. M. Vitomirov, S. B. Anderson, and J. H. Weaver, *Phys. Rev. B* **34**, 6605 (1986).
- ²⁵S. D. Bader, *J. Magn. Magn. Mater.* **100**, 440 (1991).
- ²⁶A. C. Durst, Y. B. Xu, and J. A. C. Bland (unpublished).
- ²⁷I. M. L. Billas, A. Chatelain, and W. A. de Heer, *Science* **265**, 1682 (1994).
- ²⁸J. Shi, S. Gider, K. Babcock, and D. D. Awschalom, *Science* **271**, 937 (1996).
- ²⁹C. P. Bean and J. D. Livingston, *J. Appl. Phys.* **30**, 120 (1959).
- ³⁰V. Pokrovskii, *Adv. Phys.* **28**, 595 (1979).
- ³¹R. Skomski, D. Sander, J. Shen, and J. Kirschner, *J. Appl. Phys.* **81**, 4710 (1997).
- ³²E. Gu, J. A. C. Bland, C. Daboo, M. Gester, L. M. Brown, R. Ploessl, and J. N. Chapman, *Phys. Rev. B* **51**, 3596 (1995).

- ³³R. B. Stinchcombe, in *Phase Transitions and Critical Phenomena*, edited by C. Domb and J. L. Lebowitz (Academic, London, 1983).
- ³⁴F. O. Schumann and J. A. C. Bland, *J. Appl. Phys.* **73**, 5945 (1993).
- ³⁵G. W. Anderson, M. C. Hanf, X. R. Qin, P. R. Norton, K. Myrtle, and B. Heinrich, *Surf. Sci.* **346**, 145 (1996).
- ³⁶A. Zangwill, *Physics at Surface* (Cambridge University Press, Cambridge, England, 1988).
- ³⁷F. O. Schumann, M. E. Buckley, and J. A. C. Bland, *Phys. Rev. B* **50**, 16 424 (1995).
- ³⁸J. Shen, R. Skomski, M. Klaua, H. Jenniches, S. S. Manoharan, and J. Kirschner, *Phys. Rev. B* **56**, 2340 (1997).
- ³⁹I. P. Smorchkova, N. Samarth, J. M. Kikkawa, and D. D. Awschalom, *Phys. Rev. Lett.* **78**, 3571 (1997).
- ⁴⁰A. Nogaret, S. Carlton, B. L. Gallagher, P. C. Main, M. Henini, R. Wirtz, R. Newbury, M. A. Howson, and S. P. Beaumont, *Phys. Rev. B* **55**, R16 037 (1997).